International Journal of Engineering Trends and Technology
ISSN: 2231 – 5381 /doi:10.14445/22315381/IJETT-V69I4P209

Volume 69 Issue 4, 57-66, April 2021

A Refined Theory for Bending Vibratory Analysis of Thick Functionally Graded-Beams

Zakaria Ibnorachid[#1], Lhoucine Boutahar[*2], Khalid El bikri[#3]

[#*]*Mohammed V University in Rabat, ENSAM,M2SM, BP 6207, Rabat Institus, Rabat, Morocco*

[1]ibnorachid@gmail.com, [2]lhoucine.boutahar@um5s.net.ma , [3]k.elbikri@um5s.net.ma

Abstract *- A refined beam-theory taking a count the thickness-stretching is presented in this research for bending vibratory behavior analysis of thick FG-beams. In this theory, the number of unknowns is reduced to four instead of five in the other theories. Transverse displacement is expressed through a hyperbolic function and subdivided into bending, shear, and thickness-stretching components. The number of unknowns is so reduced, which involves a decrease of the governing equations number. The boundary conditions at the top and bottom FG-beam faces are satisfied without any shear correction factor. Effective characteristics of FG-beam material change continuously in the thickness direction according to a distribution law depending on the constituents volume proportion. Equations of motion are obtained from Hamilton's principle and are solved by assuming the Navier's solution type, for the case of a Simply Supported FG-beam, transversely loaded. Numerical results obtained are exposed and analyzed in detail to verify the validity of the current theory and to prove the influence of the material composition, geometry, shear, and normal deformation on the frequency response and stresses.*

Keywords: *Refined beam-theory, Functionally Graded Beam, Thickness stretching.*

I. INTRODUCTION

Functionally classified FGMs are new types of composites obtained by mixing ceramic and metallic constituents [1]. Material properties vary continuously through the beam-thickness in the function of the mixing proportion. This avoids the stress concentration observed in laminate composites. MGFs are reserved for specific uses, for example, coatings of thermal barriers for turbine blades, shielding for military applications, automotive, space, and aerospace industries, biomedical materials.

FGMs are currently in great demand by industries, so they require very specific models to analyze their behavior and predict their responses. Many researchers have been interested in different analyzes of the FGM structures because of their wide application areas. Both main beam models, the Euler-Bernoulli model (CBT) for thin beams and the Timoshenko model (SDT) for thick beams, were introduced. CBT model ignores the transverse shear deformation effect. It was modified to take into account the shear deformation into consideration, resulting in the SDT model. But, this second model requires a shear correction to satisfy the boundary conditions on the top and bottom beam faces, which influences the results. The Higher-order SDT aims to eliminate the failure of CBT and First-order SDT by assuming a higher-order variation through FG-B thickness for transverse displacement without providing any shear correction.

Multiple models with various shear stress shapes have been proposed, for example, the Reddy model [2]. Thai and VO [3] have presented several refined theories of HSDT beams. They have shown that these models are very effective in the static and dynamic studies of FG and laminates beams. Recently, Ibnorachid et al. [4] investigated thermo-mechanical behavior of Porous Functionally Graded Beams, resting on elastic foundations by using a Refined HSDT. Aydogdu and Taskin [5] used the Euler Bernoulli model and parabolic and exponential shear functions to examine the bending vibration-responses of a Simply-Supported FG-Beams. Sallai et al. [6] used different beam theories to investigate the static behavior of an FG thick Timoshenko-beam. A numerical solution for (TBT) and (HSDT) is presented by Simsek [7] using the Ritz method. The finite element method and HSDT are used by Kadoli et al. [8] to analyze the bending vibration responses of the thick FG-beams. An analytical solution for the cantilevered thick FG-beams is provided by Zhong and Yu [9] for various types of mechanical loads. Based on the neutral surface concept, Ould Larbi [10] presented an efficient theory to study bending-free vibration of thick FG-beams. Similarly, a new First order of SDT theory is developed by Bouremana et al. [11], based on the position of the neutral surface for thick FG-beams.

The thickness-stretching impact was introduced for the first time in the analysis of the vibrational behavior of thick FG plates [12-14]. Ibnorachid et al. [15] studied the free and forced vibration behavior of simply supported FG beams using an HSDT in which the thickness-stretching effect is incorporated. Osofero et al. [16] provided an analysis method of buckling in bending of FG sandwich beams, considering thickness-stretching and shear effects. Meradjah et al. [17] also integrated the thickness-stretching effects in a new shear strain theory that they proposed to analyze the bending vibration of FG-beams.

A refined theory is presented in this work to analyze bending vibration of thick FG-beam, with simply supported ends and under transverse loading. By superimposing the deflection on the bending, shear, and thickness-stretching parts, the governing equations are derived from Hamilton's principle. The equations system obtained is solved by using Navier's solutions. The material characteristics are presumed to change through the beam thickness following the law of dosing. Detailed mathematical formulations are provided, and example results are proposed to show the relevance of the present theory to other theories using more unknowns and to prove the effects of thickness-stretching and the influences of many parameters such as material index and slenderness ratio on frequency response and stresses.

II. THEORETICAL FORMULATION

A. Model definition

Fig.1 shows the proposed model for this study. It is a thick FG-beam with length (L), of the rectangular section having for width (b) and for height (h).

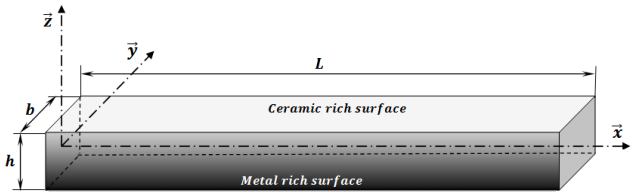

Fig. 1 Geometry of the FG-beam

The FG-beam is composed of a combination of metal and ceramics whose combination changes from the top surface purely ceramic to the bottom surface completely metallic. The beam material effective characteristic $\mathcal{P}$ is assumed to de changes through the FG-beam thickness in relation to the volume ratio and the characteristics of the constituent material. It is formulated by the law of mixing as follow:

$$\mathcal{P} = \mathcal{P}_m \vartheta_m + \mathcal{P}_c \vartheta_c \ , \qquad \mathcal{P} = (E, \rho, \nu, \dots\dots) \tag{1}$$

E, ρ, ν are Young modulus, mass density, and Poisson's coefficient, respectively. Variation of ν is generally small, so it remains constant.

$\vartheta_c$and ϑ_m are ceramic and metal volume proportions respectively, defined by [18]:

$$\vartheta_m + \vartheta_c = 1, \quad \vartheta_c = \left(0.5 + {}^{z}/_{h}\right)^{p}, \qquad p \geq 0 \tag{2}$$

The gradient index(p), with $p \geq 0$, determines the profile of the material in the FG beam thickness direction. It can be modified to obtain the optimum component materials distribution.

The plot in Fig.2 shows the distribution of ceramic volume proportion across the FG-beam thickness for different values of the material indexes.

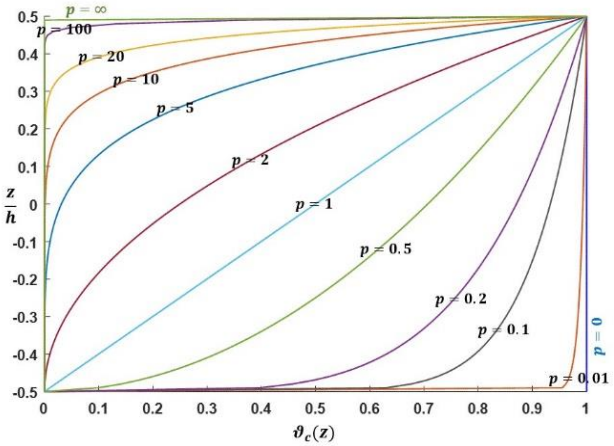

Fig. 2 Ceramic volume proportion profile across FG-beam thickness for different values of p

Each effective characteristic of the FG-beam can be expressed as follows:

$$\mathcal{P}(z) = (\mathcal{P}_c - \mathcal{P}_m)\left(0.5 + {}^{z}/_{h}\right)^{p} + \mathcal{P}_m \ , \qquad \mathcal{P} = E, \rho \tag{3}$$

B. Displacement and strain fields

Transverse and axial displacements of the FG-structure are expressed, according to the casi-3D theory [19], as follow:

$$\begin{cases} U(x,z) = u_0(x) - z\,\partial w_b/\partial x - \digamma(z)\,\partial w_s/\partial x \\ W(x,z) = w_b(x) + w(x) + w_{st}(x) \end{cases} \tag{4}$$

with,

$$w_{st}(x) = \gimel(z)\phi(x), \quad \gimel(z) = 1 - d\digamma(z)/dz \tag{5}$$

u_0 : Axial displacement
w_b : Bending transverse displacement
w_s : Shear transverse displacement
w_{st}: Thickness-Stretching displacement
u_0, w_b, w_s and $\phi$are four unknowns to be determined
$\digamma(z)$ and $\gimel(z)$are the shape functions
The strains are as follows:

$$\begin{cases} \varepsilon_x = \partial u_0/\partial x - z\,\partial^2 w_b/\partial x^2 - \digamma(z)\,\partial^2 w_s/\partial x^2 \\ \varepsilon_z = (d\gimel(z)/dz)\phi \\ \gamma_{xz} = \gimel(z)[\partial w_s/\partial x + \partial\phi/\partial x] \end{cases} \tag{6}$$

The FG-beam material obeys Hooke's law. So, the linear elastic equation can be expressed as:

$$\begin{Bmatrix}\sigma_x\\ \sigma_z\\ \tau_{xz}\end{Bmatrix} = \mathrm{E(z)}\begin{bmatrix}1 & \nu & 0\\ \nu & 1 & 0\\ 0 & 0 & \dfrac{1}{2(1+\nu)}\end{bmatrix}\begin{Bmatrix}\varepsilon_x\\ \varepsilon_z\\ \gamma_{xz}\end{Bmatrix}$$

$$= E(z)\begin{Bmatrix}\dfrac{\partial u_0}{\partial x} - z\dfrac{\partial^2 w_b}{\partial x^2} - \text{ff}(z)\dfrac{\partial^2 w_s}{\partial x^2} + \nu\dfrac{d\text{g}(z)}{dz}\phi\\ \nu\dfrac{\partial u_0}{\partial x} - \nu z\dfrac{\partial^2 w_b}{\partial x^2} - \nu\text{ff}(z)\dfrac{\partial^2 w_s}{\partial x^2} + \dfrac{d\text{g}(z)}{dz}\phi\\ \dfrac{1}{2(1+\nu)}\left(\dfrac{\partial w_b}{\partial x} + \dfrac{\partial w_s}{\partial x}\right)\end{Bmatrix} \quad (7)$$

C. Calculation of energies

*1) **Strain energy***

$$\begin{cases}\delta\mathcal{U} = \displaystyle\int_0^L\int_0^b\left[\int_{-\frac{h}{2}}^{\frac{h}{2}}\begin{pmatrix}\sigma_x\delta\varepsilon_x\\ +\tau_{xz}\delta\gamma_{xz} + \sigma_z\delta\varepsilon_z\end{pmatrix}dz\right]dydx\\ \quad = \displaystyle\int_0^L\begin{pmatrix}\mathcal{N}_x\dfrac{\partial\delta u_0}{\partial x} - \mathcal{M}_x^b\dfrac{\partial^2\delta w_b}{\partial x^2} - \mathcal{M}_x^s\dfrac{\partial^2\delta w_s}{\partial x^2}\\ +\mathcal{Q}_{xz}\left(\dfrac{\partial\delta w_s}{\partial x} + \dfrac{\partial\delta\phi}{\partial x}\right) + \mathcal{N}_z\delta\phi\end{pmatrix}dx\end{cases} \quad (8)$$

where, $\mathcal{N}_x$, $\mathcal{M}_x^b$, $\mathcal{M}_x^s$, $\mathcal{Q}_{xz}$ and $\mathcal{N}_z$ are the stress resultants, specified as:

$$\begin{cases}(\mathcal{N}_x, \mathcal{M}_x^b, \mathcal{M}_x^s) = \displaystyle\int_{-h/2}^{h/2}[1, z, \text{ff}(z)]\sigma_x\, b\, dz\\ \mathcal{Q}_{xz} = \displaystyle\int_{-h/2}^{h/2}\tau_{xz}\text{g}(z) b\, dz\\ \mathcal{N}_z = \displaystyle\int_{-h/2}^{h/2}\sigma_z\frac{d\text{g}(z)}{dz} b\, dz\end{cases} \quad (9)$$

By using Eq (7), the stress resultants given in Eq (9) can be expressed as:

$$\begin{Bmatrix}\mathcal{N}_x\\ \mathcal{M}_x^b\\ \mathcal{M}_x^s\\ \mathcal{Q}_{xz}\\ \mathcal{N}_z\end{Bmatrix} = \begin{bmatrix}\mathcal{A} & \mathcal{B} & \mathcal{B}_s & \mathcal{X} & 0\\ \mathcal{B} & \mathcal{D} & \mathcal{D}_s & \mathcal{Y} & 0\\ \mathcal{B}_s & \mathcal{D}_s & \mathcal{H}_s & \mathcal{Y}_s & 0\\ \mathcal{X} & \mathcal{Y} & \mathcal{Y}_s & \mathcal{Z} & 0\\ 0 & 0 & 0 & 0 & \mathcal{A}_s\end{bmatrix}\begin{Bmatrix}\dfrac{\partial u_0}{\partial x}\\ -\dfrac{\partial^2 w_b}{\partial x^2}\\ -\dfrac{\partial^2 w_s}{\partial x^2}\\ \left(\dfrac{\partial w_s}{\partial x} + \dfrac{\partial\phi}{\partial x}\right)\end{Bmatrix} \quad (10)$$

$(\mathcal{A}, \mathcal{B}, \mathcal{D}, \mathcal{B}_s, \mathcal{D}_s, \mathcal{H}_s, \mathcal{X}, \mathcal{Y}, \mathcal{Y}_s, \mathcal{Z}, \mathcal{A}_s)$ are the FG-beam stiffness expressed as follows:

$$\begin{cases}(\mathcal{A}, \mathcal{B}, \mathcal{D}, \mathcal{B}_s, \mathcal{D}_s, \mathcal{H}_s) = \\ \quad \displaystyle\int_{-h/2}^{h/2}(1, z, z^2, \text{ff}(z), z\text{ff}(z), \text{ff}(z)^2)E(z)\, b\, dz\\ (\mathcal{X}, \mathcal{Y}, \mathcal{Y}_s, \mathcal{Z}) = \\ \quad \displaystyle\int_{-h/2}^{h/2}\left(\nu, \nu z, \nu\text{ff}(z), \frac{d\text{g}(z)}{dz}\right)\frac{d\text{g}(z)}{dz}E(z)\, b\, dz\\ \mathcal{A}_s = \displaystyle\int_{-h/2}^{h/2}\text{g}(z)^2\frac{E(z)}{2(1+\nu)}bdz\end{cases} \quad (11)$$

*2) **Potential energy due to the external transverse load applied***

$$\delta\mathcal{V} = -\int_0^L q(x)\delta W dx = -\int_0^L q(x)\delta(w_b + w_s + w_{st})dx \quad (12)$$

q(x): External transverse loading.

*3) **Kinetic energy***

$$\begin{cases}\delta\mathcal{K} = \displaystyle\int_0^L\int_0^b\left[\int_{-h/2}^{h/2}\rho(z)\left(\dot{U}\delta\dot{U} + \dot{W}\delta\dot{W}\right)dz\right]dydx\\ \quad = \displaystyle\int_0^L\begin{pmatrix}I_0[\dot{u}_0\delta\dot{u}_0 + (\dot{w}_b + \dot{w}_s)(\delta\dot{w}_b + \delta\dot{w}_s)]\\ +J_0\left[(\dot{w}_b + \dot{w}_s)\delta\dot{\phi} + \dot{\phi}\delta(\dot{w}_b + \dot{w}_s)\right]\end{pmatrix}dx\\ -\displaystyle\int_0^L\begin{pmatrix}I_1\left[\dot{u}_0\dfrac{\partial\delta\dot{w}_b}{\partial x} + \dfrac{\partial\dot{w}_b}{\partial x}\delta\dot{u}_0\right] + I_2\dfrac{\partial\dot{w}_b}{\partial x}\dfrac{\partial\delta\dot{w}_b}{\partial x}\\ +J_1\left[\dot{u}_0\dfrac{\partial\delta\dot{w}_s}{\partial x} + \dfrac{\partial\dot{w}_s}{\partial x}\delta\dot{u}_0\right]\end{pmatrix}dx\\ -\displaystyle\int_0^L\begin{pmatrix}K_2\dfrac{\partial\dot{w}_s}{\partial x}\dfrac{\partial\delta\dot{w}_s}{\partial x} - J_2\left[\dfrac{\partial\dot{w}_b}{\partial x}\dfrac{\partial\delta\dot{w}_s}{\partial x} + \dfrac{\partial\dot{w}_s}{\partial x}\dfrac{\partial\delta\dot{w}_b}{\partial x}\right]\\ +K_0\dot{\phi}\delta\dot{\phi}\end{pmatrix}dx\end{cases} \quad (13)$$

$(I_0, I_1, I_2, J_0, J_1, J_2, K_0, K_2)$ are the mass inertias, defined as follows:

$$\begin{cases}(I_0, I_1, I_2) = \displaystyle\int_{-h/2}^{h/2}(1, z, z^2)\rho(z)\, b\, dz\\ (J_0, J_1, J_2) = \displaystyle\int_{-h/2}^{h/2}(\text{g}, \text{ff}(z), z\text{ff}(z))\rho(z)\, b\, dz\\ (K_0, K_2) = \displaystyle\int_{-h/2}^{h/2}(\text{g}(z)^2, \text{ff}(z)^2)\rho(z)\, b\, dz\end{cases} \quad (14)$$

D. Governing equation

To obtain the beam governing-equation, Hamilton principle is applied as follows.

$$\int_{t1}^{t2}(\delta\mathcal{U} + \delta\mathcal{V} - \delta\mathcal{K})\mathrm{dt} = 0 \quad (15)$$

Replacing the expressions $\delta\mathcal{U}, \delta\mathcal{V}$ and $\delta\mathcal{K}$ of Eqs (8),(12) and (13) into Eq (15), we obtain the following system by integrating by parts, and by gathering the coefficients of $\delta u_0, \delta w_b, \delta w_s$ and $\delta\phi$.

$$\begin{cases} \delta u_0 : \dfrac{\partial \mathcal{N}_x}{\partial x} = I_0 \ddot{u}_0 - I_1 \dfrac{\partial \ddot{w}_b}{\partial x} - J_1 \dfrac{\partial \ddot{w}_s}{\partial x} \\ \delta w_b : \dfrac{\partial^2 \mathcal{M}_x^b}{\partial x^2} + q = I_0(\ddot{w}_b + \ddot{w}_s) \\ \quad + I_1 \dfrac{\partial \ddot{u}_0}{\partial x} - I_2 \dfrac{\partial^2 \ddot{w}_b}{\partial x^2} - J_2 \dfrac{\partial^2 \ddot{w}_s}{\partial x^2} + J_0 \ddot{\phi} \\ \delta w_s : \dfrac{\partial^2 \mathcal{M}_x^s}{\partial x^2} + \dfrac{\partial Q_{xz}}{\partial x} + q = I_0(\ddot{w}_b + \ddot{w}_s) \\ \quad + J_1 \dfrac{\partial \ddot{u}_0}{\partial x} - J_2 \dfrac{\partial^2 \ddot{w}_b}{\partial x^2} - K_2 \dfrac{\partial^2 \ddot{w}_s}{\partial x^2} + J_0 \ddot{\phi} \\ \delta \phi : \dfrac{\partial Q_{xz}}{\partial x} - \mathcal{N}_z = J_0(\ddot{w}_b + \ddot{w}_s) + K_0 \ddot{\phi} \end{cases} \tag{17}$$

Using Eq (10) we can express Eqs (17) in terms of displacement of u_0, w_b, w_s and ϕ as follows:

$$\begin{cases} \delta u_0 : \mathcal{A} \dfrac{\partial^2 u_0}{\partial x^2} - \mathcal{B} \dfrac{\partial^3 w_b}{\partial x^3} - \mathcal{B}_s \dfrac{\partial^3 w_s}{\partial x^4} + \mathcal{X} \dfrac{\partial \phi}{\partial x} \\ \quad = I_0 \ddot{u}_0 - I_1 \dfrac{\partial \ddot{w}_b}{\partial x} - J_1 \dfrac{\partial \ddot{w}_s}{\partial x} \\ \delta w_b : \mathcal{B} \dfrac{\partial^3 u_0}{\partial x^3} - \mathcal{D} \dfrac{\partial^4 w_b}{\partial x^4} - \mathcal{D}_s \dfrac{\partial^4 w_s}{\partial x^4} + \mathcal{Y} \dfrac{\partial^2 \phi}{\partial x^2} + q \\ \quad = I_1 \dfrac{\partial \ddot{u}_0}{\partial x} + I_0(\ddot{w}_b + \ddot{w}_s) - I_2 \dfrac{\partial^2 \ddot{w}_b}{\partial x^2} \\ \quad - J_2 \dfrac{\partial^2 \ddot{w}_s}{\partial x^2} + J_0 \ddot{\phi} \\ \delta w_s : \mathcal{B}_s \dfrac{\partial^3 u_0}{\partial x^3} - \mathcal{D}_s \dfrac{\partial^4 w_b}{\partial x^4} - \mathcal{H}_s \dfrac{\partial^4 w_s}{\partial x^4} + \mathcal{A}_s \dfrac{\partial^2 w_s}{\partial x^2} \\ \quad + (\mathcal{A}_s + \mathcal{Y}_s) \dfrac{\partial^2 \phi}{\partial x^2} + q = J_1 \dfrac{\partial \ddot{u}_0}{\partial x} + I_0(\ddot{w}_b + \ddot{w}_s) \\ \quad - J_2 \dfrac{\partial^2 \ddot{w}_b}{\partial x^2} - K_2 \dfrac{\partial^2 \ddot{w}_s}{\partial x^2} + J_0 \ddot{\phi} \\ \delta \phi : \mathcal{X} \dfrac{\partial u_0}{\partial x} - \mathcal{Y} \dfrac{\partial^2 w_b}{\partial x^2} + (\mathcal{A}_s + \mathcal{Y}_s) \dfrac{\partial^2 w_s}{\partial x^2} \\ \quad - \mathcal{A}_s \dfrac{\partial^2 \phi}{\partial x^2} + \mathcal{Z} \phi = J_0(\ddot{w}_b + \ddot{w}_s) + K_0 \ddot{\phi} \end{cases} \tag{18}$$

E. Analytical solution for a Simple Supported Functionally Graded beam (S-S FG-beam)

Analytical solutions of the motion equations are provided, based on Navier type solutions. The following displacements u_0, w_b, w_s and ϕ are assumed to be combinations of known trigonometric functions which satisfy the boundary conditions. The unknown coefficients are determined for each "n".

$$\begin{bmatrix} u_0(x,t) \\ w_b(x,t) \\ w_s(x,t) \\ \phi(x,t) \end{bmatrix} = \sum_{n=1}^{\infty} \begin{bmatrix} U_n \cos(\lambda x) e^{i\omega_n t} \\ W_{bn} \sin(\lambda x) e^{i\omega_n t} \\ W_{sn} \sin(\lambda x) e^{i\omega_n t} \\ \phi_n \sin(\lambda x) e^{i\omega_n t} \end{bmatrix} \tag{19}$$

$\omega_n$is the eigen frequency associated with the n^{th}eigen mode, $\lambda = n\pi/L$, and U_n, W_{bn}, W_{sn} and ϕ_n are the unknown coefficients.

The following boundary conditions are imposed for a beam with two ends simply supported.

$$U = W = \mathcal{M}_x^b = \mathcal{M}_x^s = 0 \tag{20}$$

The assumed mechanical transverse load $q(x)$ is developed in a sinusoidal Fourier series as:

$$q(x) = \sum_{n=1}^{\infty} Q_n \sin(\lambda x) \tag{21}$$

We give for certain loads, the following coefficients Q_n.

1) ***Sinusoidal distribution case:***

$$n = 1 \Longrightarrow Q_1 = q_0 \tag{22}$$

2) ***Uniform distributioncase:***

$$Q_n = \frac{4q_0}{n\pi}, \quad (n = 1, 3, 5) \tag{23}$$

Analytical solutions may be reached from the eigenvalues system below for any fixed value of "n":

$$([K] - \omega_n^2[M])\{\Delta\} = \{F\} \tag{24}$$

In the static problem case, Eq.(24)becomes:

$$[K]\{\Delta\} = \{F\} \tag{25}$$

with,

$$[K] = \begin{bmatrix} k_{11} & k_{12} & k_{13} & k_{14} \\ k_{12} & k_{22} & k_{23} & k_{24} \\ k_{13} & k_{11} & k_{33} & k_{34} \\ k_{14} & k_{24} & k_{34} & k_{44} \end{bmatrix};$$

$$[M] = \begin{bmatrix} m_{11} & m_{12} & m_{13} & 0 \\ m_{12} & m_{22} & m_{23} & m_{24} \\ m_{13} & m_{23} & m_{33} & m_{34} \\ 0 & m_{24} & m_{34} & m_{44} \end{bmatrix}; \tag{26}$$

$$\{\Delta\} = \begin{Bmatrix} U_n \\ W_{bn} \\ W_{sn} \\ \phi_n \end{Bmatrix}, \qquad \{F\} = \begin{Bmatrix} 0 \\ Q_n \\ Q_n \\ 0 \end{Bmatrix}$$

$$\begin{aligned} &k_{11} = \mathcal{A}\lambda^2;\ k_{12} = -\mathcal{B}\lambda^3;\ k_{23} = \mathcal{D}_{11}^s\lambda^4; \\ &k_{22} = \mathcal{D}_{11}\lambda^4;\ k_{13} = -\mathcal{B}_s\lambda^3;\ k_{24} = \mathcal{Y}\lambda^2; \\ &k_{33} = \mathcal{H}\lambda^4 + \mathcal{A}_s\lambda^2;\ k_{14} = -\mathcal{X}\lambda; \\ &k_{34} = (\mathcal{A}_s + \mathcal{Y}_s)\lambda^2;\ k_{44} = \mathcal{Z} + \mathcal{A}_s\lambda^2; \\ &m_{11} = I_0;\ m_{12} = -I_1\lambda;\ m_{13} = -J_1\lambda; \\ &m_{22} = I_0 + I_2\lambda^2;\ \ m_{23} = I_0 + J_2\lambda^2;\ m_{24} = J_0; \\ &m_{33} = I_0 + K_2\lambda^2;\ m_{34} = J_0;\ m_{44} = K_0 \end{aligned} \tag{27}$$

III. NUMERICAL RESULTS AND DISCUSSION

In this part, a uniform transverse load is applied to the FG S-S FG-beam. Some numerical examples are proposed to first validated the model presented above and assess its accuracy. The FG-beam material is composed by Al_2O_3(Alumina) and Al(Aluminum). The material

characteristics of the corresponding components are listed in Table1.

TABLE I. Material characteristics of $Al_2O_3$and Al [21]

Components	ν	$E(GPa)$	$\rho\ (kg/m^3)$
Ceramic (alumina Al_2O_3)	0.3	380	3960
Metal (aluminum Al)	0.3	70	2702

Dimensionless form is used as follows:

$$\bar{U} = 100\left(\frac{E_m h^3}{q_0 L^4}\right) U\left(0, -\frac{h}{2}\right);$$
$$\overline{W} = 100\left(\frac{E_m h^3}{q_0 L^4}\right) W(L/2, h/2)$$
$$\overline{\sigma_{xz}} = \left(\frac{h}{q_0 L}\right)\sigma_{xz}(0,0); \quad \bar{\sigma}_z = \left(\frac{h}{q_0 L}\right)\sigma_z\left(\frac{L}{2}, \frac{h}{2}\right); \tag{28}$$
$$\bar{\omega} = (\omega L^2/h)\sqrt{\frac{\rho_m}{E_m}}$$

Numerical example as set out in Table 2 is performed for various material indexes to validate the present model. The results obtained by this theory, concerning displacements and the stresses, for (L/h=5) and those obtained by the analytical solution provided by Li et al. [22] are compared. The following shape function on the basis of Reddy beam theory is used:

$$f(z) = \frac{4z^3}{3h^2} \tag{29}$$

A. Static analysis

TABLE II reveals that the présent théory is agree perfectly with that of Li et al. [22], and thus confirme the validation of the proposed method of solution. It can be seen also that the CBT model, wich omits shear deformation effects, under-estimates displacements and stresses of the thick FG-beams.

TABLE II. Comparison of Non- dimensional transverse and axial displacements, axial and shear stresses of S-S FG-beam for various material indexes

p	Theory	$L/h = 5$			
		$\overline{W}$	$\bar{U}$	$\bar{\sigma}_x$	$\bar{\sigma}_{xz}$
0	Li et al. [22]	3.1657	0.9402	3.8020	0.7500
	CBT	2.8783	0.9211	3.7500	-
	Present	3.1681	0.9406	3.7919	0.7503
0.5	Li et al. [23]	4.8292	1.6603	4.9925	0.7676
	CBT	4.4401	1.6331	4.9206	-
	Present	4.8202	1.6653	4.9893	0.7674
1	Li et al. [23]	6.2599	2.3045	5.8837	0.7500
	CBT	5.7746	2.2722	5.7959	-
	Present	6.2475	2.2903	5.8797	0.7503
5	Li et al. [23]	9.7802	3.7089	8.1030	0.5790
	CBT	8.7508	3.6496	8.1329	-
	Present	9.7787	3.6955	8.1099	0.5867
10	Li et al. [23]	10.8979	3.8860	9.7063	0.6436
	CBT	9.6072	3.8097	9.5228	-
	Present	10.8847	3.8780	9.7086	0.6645

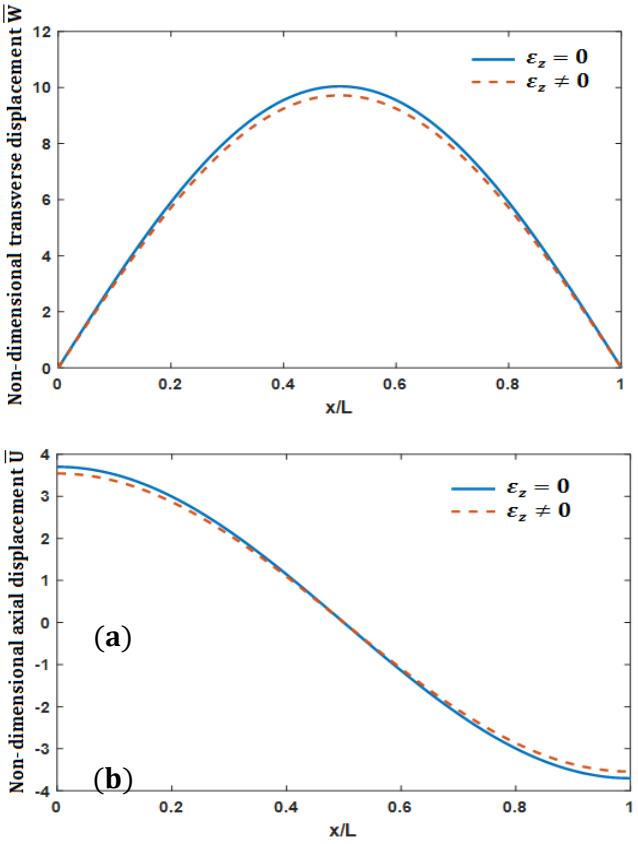

Fig. 3 Thickness stretching effect on the non-dimensional: (a)transverse, (b)axial displacements

To investigate again the effects of the thickness stretching on displacements, a comparison between the non dimensional displacements of the beam obtained from the present model with and without thickness stretching is made in Figs.3 (a) and (b) for the transverse and axial displacements respectively, for (L/h=5) and (p=5). The difference between the two curves is clearly seen. It is large out in the midle of the beam and becomes zero at the ends for the transverse displacement and becomes zero out in the middle of the beam for the axial displacement, unlike for the axial displacement wich is large at the ends and vanishes out in the midle of the beam.

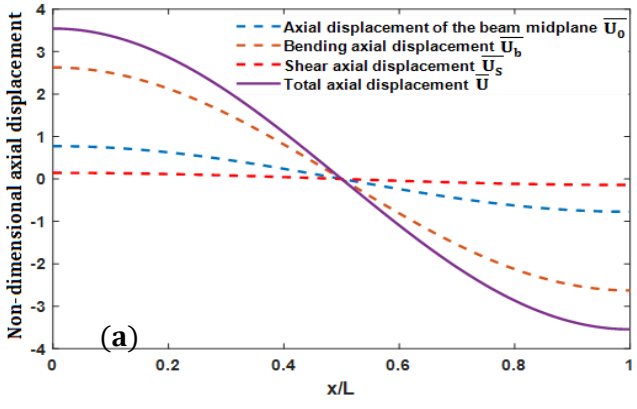

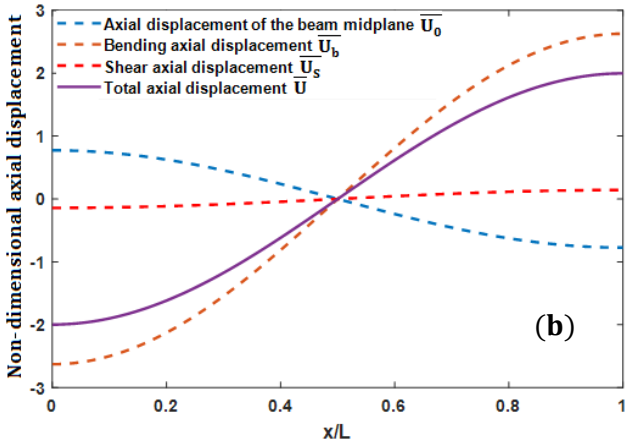

Fig. 4 Shear effect on axial displacement a long of the FGB on: (a) Lower beam face and (b) Uper beam face.

Effect of shear on the évolution of non-dimensional axial displacement along the beam on the uper and lower beam faces is evaluated from Fig. 4, for (L/h=5) and (p=5). It's clearly that shear does not have a great effect on the axial displacement, but not negligible. It can be seen also that shear it is maximum at the ends and vanishes at mid-span of the beam.

In second examination and analysis example, effects of shear and thickness stretching on the non-dimensional tranverse displacement of the FG S-S beam are evaluated in Fig. 5, for (L/h=5) and (p=5). It is obvious from these figures that the shear effect is more important on the two displacements and it is greatest than the effect of thickness streching for the transverse displacement. So the effect of the shear on the displacements connot be overlooked, especially for the thick beams.

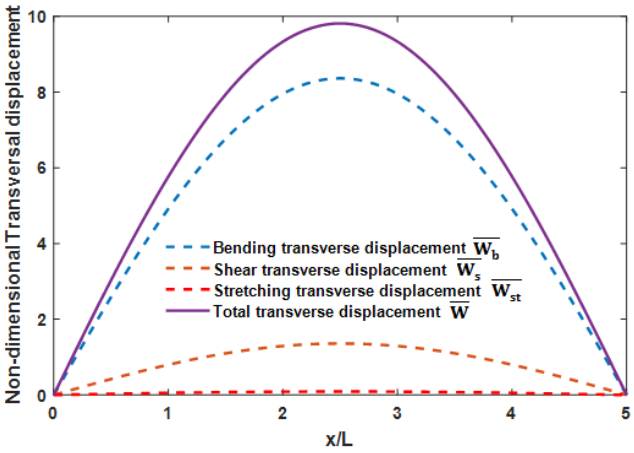

Fig. 5 Shear and stretching effects on the transverse displacement.

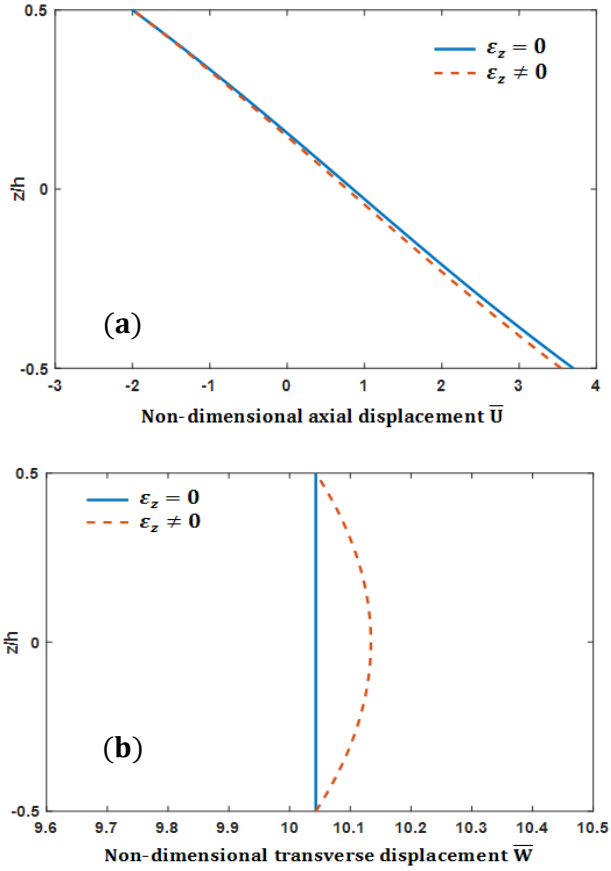

Fig. 6 Non-dimensional: (a) Axial displacement $\overline{U}$, (b) Mid-span deflection $\overline{W}$ through the FG-beam thickness.

In Figs. 6 the evolution of non-dimensional (a) in-plane displacement at the end $\overline{U}(0)$ and (b) transverse displacement $\overline{W}(L/2)$ at mid-span through the FG-beam thickness under uniform load is presented for (L/h=5) and (p=5). A slight difference appears for this shortest beam. It's clearly seen that, the maximum displacement is at the bottom of the beam for axial displacement, and at the median plane for transverse displacement. This is due to the consideration of the thickness stretching ($\varepsilon_z \neq 0$).

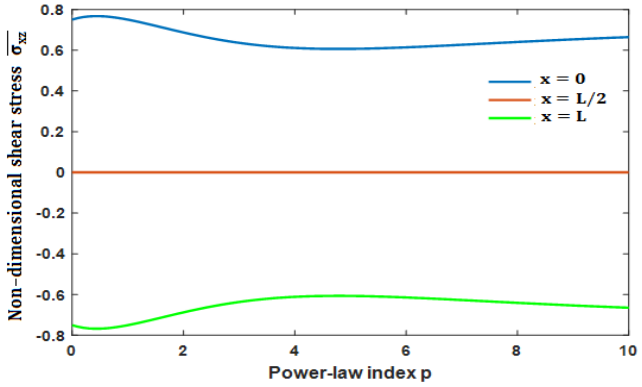

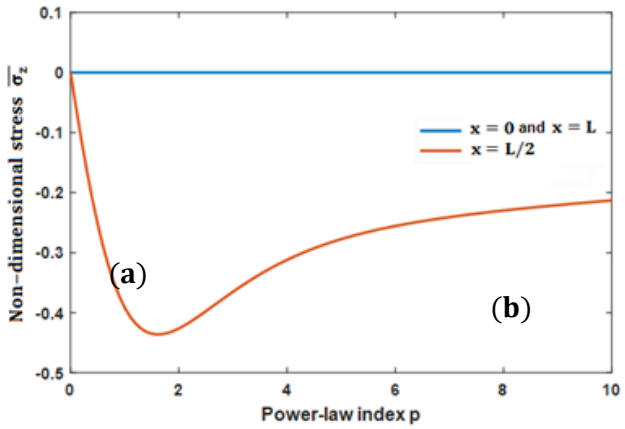

Fig. 7 Non-dimensional: (a) Shear stress $\overline{\sigma_{xz}}$, (b) stress due to the thickness stretching $\overline{\sigma_z}$ versus the material parameter.

Figs.7 (a) and (b) illustrate the evolution of the non-dimensional (a) transverse shear stress, (b) stress due to the thickness stretching, versus power-law index(p)for (L/h=5). All curves display the matérial index dependence of the stresses. It is clear that stress due to the thickness stretching exhibit low values but not negligibles compared with those of the transverse shear stress.

Variations of the non-dimensional axial stress$\overline{\sigma_x}$across the depth and versus non-dimensional length of the FGB are presented in Figs.8 (a) and (b) for (L/h=5) and (p=5). It may be seen that axial stress vanishes at the ends, but it is maximum at the middle of the beam, and The upper beam face is stretched, on the other hand, the lower face is compressed.Extension stress at the upper beam face is higher than the compressive stress at the lower face, because at uper face, the beam is ceramic-rich, whereas at the lower face, it is metal-rich. It may be observed also, that the neutral plan, where the axial stress vanishes is moved upwards relative to the middle position. This is due to non-homogeneous material of the FG-beam (p=5).

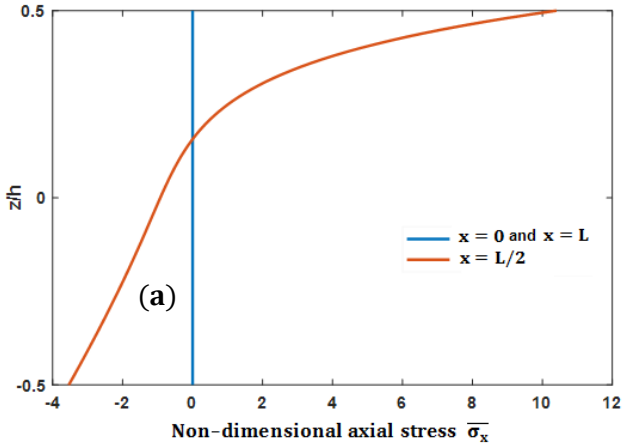

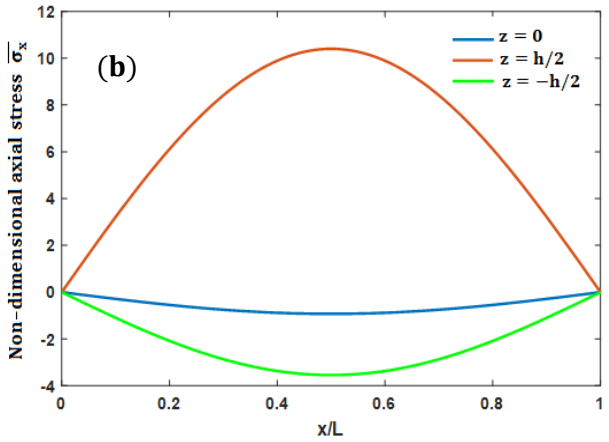

Fig. 8 $\overline{\sigma_x}$ distributions: (a)over the FG-beam thickness, (b) versus the beam non-dimensional length

In Figs.9 (a) and (b) are plotted the distributions of the non-dimensional shear stress$\overline{\sigma_{xz}}$through thethickness and versus non-dimensional length of the FG-beam, respectively, for (L/h=5) and (p=5). These figures reveal that the shear stress reaches its maximum value at the beam ends, but with opposite signs. It is canceled in the middle of the beam on the neutral plane and the lower and upper faces. As a result, the conditions of non-shearing on both lower and upper faces of the beam are satisfied.

Thickness-stretching impact on the stresses is evaluated in Figs.10 (a) and (b) for (L/h=5) and (p=5). It may be seen that $\overline{\sigma_z}$ vanishes at the ends. Its highest value is reached a midle of the beam. The upper beam face is stretched, on the other hand, the lower face is compressed. Compressive stress at the lower face of the FG-beam is higher than extension stress at the upper face.

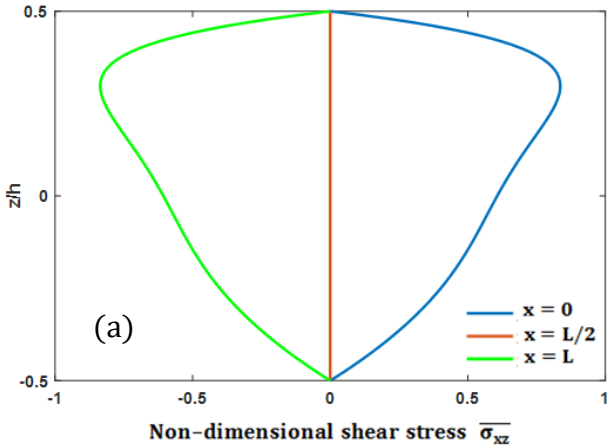

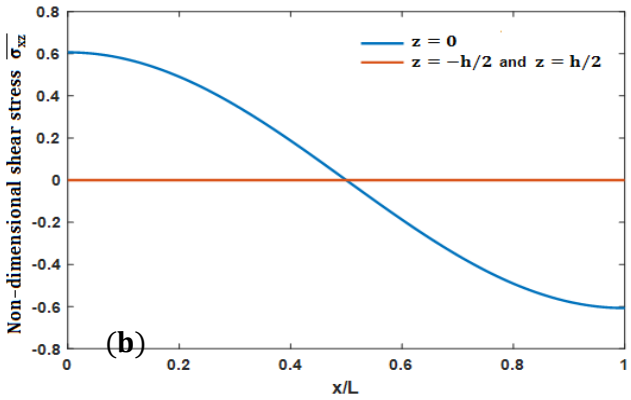

Fig 9. $\overline{\sigma_{xz}}$ Distributions: (a) over the FG-beam thickness, (b) versus dimensionneless length of the beam

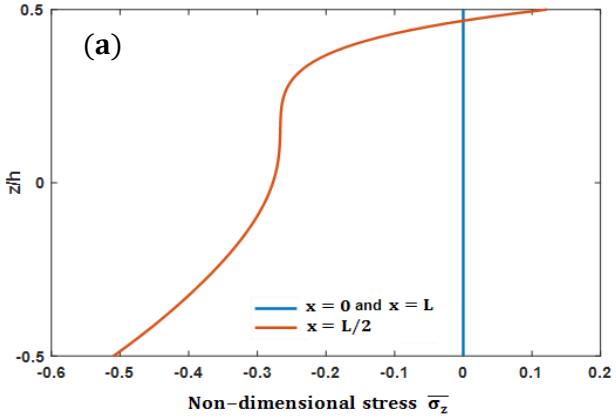

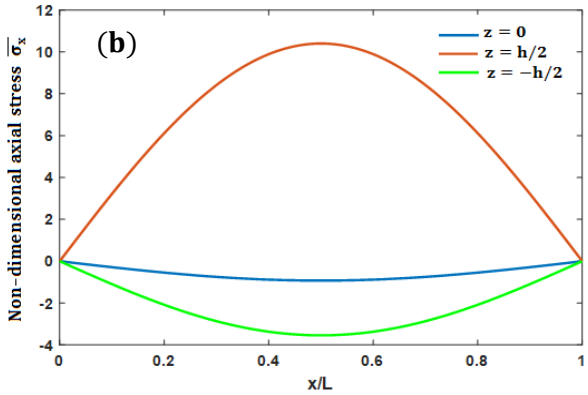

Fig 10. $\overline{\sigma_z}$ distributions: (a) over the FG-beam thickness, (b) versus the FG-beam non-dimensional length

B. Dynamic analysis

TABLE III summarizes dimensionless frequencies associated with the first, second and third mode shapes of the S-S FG-beam, for various (L/h) ratio and material parameter (p).

Again, the results obtained by the present model, when the thickness- stretching is neglected correlate closely with these obtained by the HSDT solution [10]. HSDT model under-estimates the frequencies of thick FG beams. This is due to the effect of the stretching of de the beam thickness omitted by the HSDT formulation, in the thick FG-beams case. It is emphasized that in the HSDT [10] formulation, the unknowns number is greater than this provided by the present model.

Again, the results obtained by the present model, when the thickness- stretching is neglected correlate closely with these obtained by the HSDT solution [10]. HSDT model under-estimates the frequencies of thick FG beams. This is due to the effect of the stretching of de the beam thickness omitted by the HSDT formulation, in the thick FG-beams case. It is emphasized that in the HSDT [10] formulation, the unknowns number is greater than this provided by the present model.

Dimensionless frequency variation versus material parameter for a (L/h=5) with and without taking a count of the thickness stretching, is plotted in Fig11 (a). The plot shown that increasing (p) leads decrease of the frequencies. Highest frequency is achieved for (p=0, completely ceramic beam) , and the lowest for (p $\rightarrow\infty$, completely metal beam). This can be explained by the fact that the increase in (p) leads to an increase in the amount of ceramic in the mixture which is replaced by the metal, and leads to a decrease in the Young's modulus of the beam and makes it more flexible. The thickness stretching impact is shown by the offset between both curves. It is clearly seen that the frequencies are noticeably under-estimate, when thickness stretching is omited. Impact of the slenderness ratio (L/h) on the frequencies is shown in fig.11(b). It is clearly seen that increase (L/h) leads to increase of frequencies.

TABLE III: Comparison of the S-S FG-beam frequencies $\overline{\omega_1}$ for some values of (L/h) and (p)

L/h	Mode	Theory		p				
				0	**0.5**	**1**	**5**	**10**
5	**1**	**HSDT [10]**	$\varepsilon_z = 0$	5.1530	4.4110	3.9900	3.4000	3.2810
		Present	$\varepsilon_z = 0$	5.1527	4.4107	3.9904	3.4012	3.2816
			$\varepsilon_z \neq 0$	5.1516	4.4230	4.0169	3.4310	3.2984
	2	**HSDT [10]**	$\varepsilon_z = 0$	17.8840	15.4610	14.0120	11.5350	11.0220
		Present	$\varepsilon_z = 0$	17.8812	15.4588	14.0100	11.5431	11.0240
			$\varepsilon_z \neq 0$	17.8900	15.5052	14.0978	11.6348	11.0785
	3	**HSDT [10]**	$\varepsilon_z = 0$	34.2250	29.8490	27.1080	21.6990	20.7530
		Present	$\varepsilon_z = 0$	34.2097	29.8382	27.0979	21.7158	20.5561
			$\varepsilon_z \neq 0$	34.2975	29.9670	27.2813	21.8884	20.6748
20	**1**	**HSDT [10]**	$\varepsilon_z = 0$	5.4600	4.6510	4.2050	3.6480	3.5390
		Present	$\varepsilon_z = 0$	5.4603	4.6511	4.2051	3.6485	3.5390
			$\varepsilon_z \neq 0$	5.4602	4.6657	4.2351	3.6835	3.5595
	2	**HSDT [10]**	$\varepsilon_z = 0$	21.5730	18.3960	16.6340	14.3730	13.9260
		Present	$\varepsilon_z = 0$	21.5732	18.3962	16.6344	14.3746	13.9263
			$\varepsilon_z \neq 0$	21.5710	18.4520	16.7511	14.5094	14.0043
	3	**HSDT [10]**	$\varepsilon_z = 0$	47.5940	40.6530	36.7690	31.5720	30.5340
		Present	$\varepsilon_z = 0$	47.5930	40.6526	36.7679	31.5780	30.5369
			$\varepsilon_z \neq 0$	47.5841	40.7709	37.0192	31.8649	30.7005

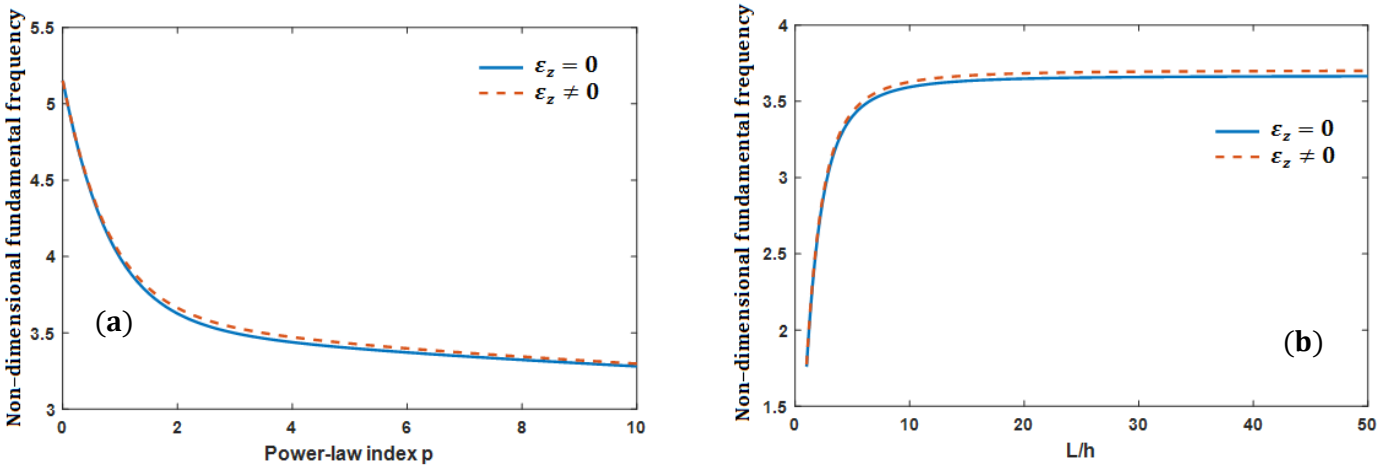

Fig.11 The Effect of the material parameter (a), beam slenderness (b), on dimensionless fundamental frequency of the S-S FG-beam.

IV. CONCLUSIONS

In this paper, a refined beam-theory is performed for bending vibratory analysis of the thick FG-beams, taking into consideration thickness-stretching.The transverse displacement is assumed to be the sum of three components, bending, shear and stretching of the thickness.This, leads to reduction of unknown's number, therefore the number of governing equations.The FG-beam effectif material characteristics are supposed change continuously in thickness direction according to a mixing law depending on volume proportion of the constituents. Governing equations are obtained from Hamilton's principle, and solved by using Navier-solutions.

Graphical and numerical results obtained here agree perfectly with those obtained using other theories with more unknowns.The effects of the thickness-stretching, impact of the material parameter and the beam-slenderness have been studied. It is clearly that the shortest beams exhibit the greatest thickness-stretching impact. Also both geometric and material parameters affect the vibrational responses of the FG-beams.

REFERENCES

[1] M. Koizumi., The concept of FGM. Cera, Trans 34 (1993) 3–10.

[2] J.N. Reddy., A simple higher-order theory for laminated composite plates, J Appl Mech, 51(4) (1984) 745–52.

[3] H.T. Thai, T. Vo., Bending and free vibration of functionally graded beams using various higher-order shear deformation beam theories, International Journal of Mechanical Sciences, 62(1) 57-66 2012.

[4] Z. Ibnorachid, L. Boutahar, K. EL Bikri, and R. Benamar., Buckling Temperature and Natural Frequencies of Thick Porous Functionally Graded Beams Resting on Elastic Foundation in a Thermal Environment, Advances in Acoustics and Vibration, (2019).Article ID 7986569.

[5] M. Aydogdu, V. Taskin., Free vibration analysis of functionally graded beams with simply supported edges, Materials & Design, 28(5) (2007) 1651-1656.

[6] B. O Sallai, A. Tounsi, I. Mechab, B. M. Bachir, M. Meradjah, B.E.A. Adda., A theoretical analysis of flexional bending of Al/Al2O3 S-FGM thick beams, Computational Materials Science, 44(4) (2009) 1344-1350.

[7] M. Şimşek., Static analysis of a functionally graded beam under a uniformly distributed load by Ritz method, Int J Eng Appl Sci, 1(3) (2009) 1-1.

[8] R. Kadoli R, K. Akhtar, N. Ganesan., Static analysis of functionally graded beams using higher order shear deformation theory, Appl Math Model, 32(12) (2008) 2509–2525.

[9] Z. Zhong Z, T. Yu., Analytical solution of a cantilever functionally graded beam, Compos Sci Technol, 67(3– 4) (2007) 481–488.

[10] L. Ould Larbi, A. Kaci A, M.S.A. Houari, A. Tounsi., An efficient shear deformation beam theory based on neutral surface position for bending and free vibration of functionally graded beams, Mech. Based Des. Struct. Machines, 41 (2013) 421–433.

[11] M. Bouremana, M.S.A. Houari, A. Tounsi, A. Kaci, E. A. Adda Bedia., A new first shear deformation beam theory based on neutral surface position for functionally graded beams, Steel Compos Struct, 15(5) (2013) 467–479.

[12] M. S. A. Houari, A. Tounsi, O. Anwar Bég., Thermoelastic bending analysis of functionally graded sandwich plates using a new higher order shear and normal deformation theory, International Journal of Mechanical Sciences, 76 (2013) 467-479.

[13] A.A. Bousahla, M. S. A. Houari, A. Tounsi, E. A. Adda Bedia., A novel higher order shear and normal deformation theory based on neutral surface position for bending analysis of advanced composite plates, International Journal of Computational Methods, 11(6) (2014) 1-18.

[14] A. Fekrar, M. S. A. Houari, A. Tounsi, S. R. Mahmoud., A new five-unknown refined theory based on neutral surface position for bending analysis of exponential graded plates, Meccanica, 49 (2014) 795-810.

[15] Ibnorachid. Z, Boutahar. L and EL Bikri. K., Free and Forced Vibration of FGM Beam Using Refined Method Including Stretching. International Journal of Advanced Research in Engineering and Technology (IJARET), 11(5) (2020) 104-115.

[16] A. Osofero, T.P. Vo, T.K. Nguyen, J. Lee., Analytical solution for vibration and buckling of functionally graded sandwich beams using various quasi-3D theories, J. Sandw. Struct. Mater, (2015).

[17] M. Meradjah, A. Kaci, M. S.A, A. Tounsi, S. R. Mahmoud., A new higher order shear and normal deformation theory for functionally graded beams, Steel Compos. Struct, 18(3) (2015) 793–809.

[18] G. N. Praveen, J. N. Reddy., Nonlinear Transient Thermo-elastic Analysis of Functionally Graded Ceramic-Metal Plates, International Journal of Solids and Structures, 35 (1998) 4457-4476.

[19] T. P. Vo, H. T Thai, T.K. Nguyen, F. Inam, J. Lee., Static behaviour of functionally graded sandwich beams using a quasi-3D theory, Composite Part B, 68 (2015) 59-74.

[20] J. N. Reddy., Energy principles and variational methods in applied mechanics, John Wiley & Sons Inc,(2002).

[21] F. Tornabene., Free vibration analysis of functionally graded conical, cylindrical shell and annular plate structures with a four-parameter power-law distribution, Comput Meth Appl Mech Eng, 198 (2009) 2911–35.

[22] X. F. Li, B.L. Wang, J. C. Han., A higher-order theory for static and dynamic analyses of functionally graded beams, Arch Appl Mech, 80(10) (2010) 1197–212.

[23] Deepak Ranjan Biswal, Alok Ranjan Biswal, Rashmi Ranjan Senapati, Finite Element Based Vibration Analysis of an Axially Functionally Graded Nonprismatic Beam SSRG International Journal of Mechanical Engineering 5(1) (2018) 8-13.